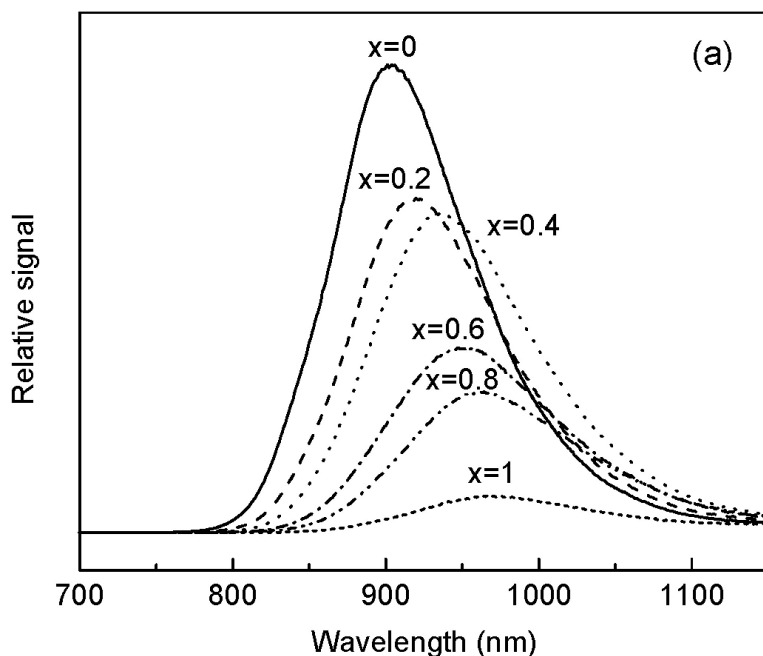


Strong Near-Infrared Luminescence in BaSnO

Hiroshi Mizoguchi, Patrick M. Woodward, Cheol-Hee Park, and Douglas A. Keszler

J. Am. Chem. Soc., **2004**, 126 (31), 9796-9800 • DOI: 10.1021/ja048866i • Publication Date (Web): 16 July 2004

Downloaded from <http://pubs.acs.org> on April 1, 2009



More About This Article

Additional resources and features associated with this article are available within the HTML version:

- Supporting Information
- Links to the 2 articles that cite this article, as of the time of this article download
- Access to high resolution figures
- Links to articles and content related to this article
- Copyright permission to reproduce figures and/or text from this article

[View the Full Text HTML](#)



ACS Publications
 High quality. High impact.

Strong Near-Infrared Luminescence in BaSnO₃

Hiroshi Mizoguchi,[†] Patrick M. Woodward,^{*,†} Cheol-Hee Park,[‡] and Douglas A. Keszler^{*,‡}

Contribution from the Department of Chemistry, The Ohio State University, 100 West 18th Avenue, Columbus, Ohio 43210-1185, and Department of Chemistry, Oregon State University, 153 Gilbert Hall, Corvallis, Oregon 97331-4003

Received February 28, 2004; E-mail: woodward@chemistry.ohio-state.edu; douglas.keszler@oregonstate.edu

Abstract: Powdered samples of the perovskite BaSnO₃ exhibit strong near-infrared (NIR) luminescence at room temperature, following band-gap excitation at 380 nm (3.26 eV). The emission spectrum is characterized by a broad band centered at 905 nm (1.4 eV), tailing on the high-energy side to approximately 760 nm. The Stokes shift is 1.9 eV, and measured lifetimes in the range 7–18 ms depend on preparative conditions. These extraordinary long values indicate that the luminescence involves a defect state(s). At low temperatures, both a sharp peak and a broad band appear in the visible portion of the luminescence spectrum at approximately 595 nm. Upon cooling, the intensity of the NIR emission decreases, while the integrated intensities of the visible emission features increase to approximately 40% of the NIR intensity at 77 K. Room-temperature photoluminescence (PL) is observed across the Ba_{1-x}Sr_xSnO₃ series. As the strontium content increases, the excitation maximum and band gap shift further into the UV, while the intensity of the NIR emission peak decreases and shifts further into the infrared. This combination leads to an unexpectedly large increase in the Stokes shift. The unusual NIR PL in BaSnO₃ may originate from recombination of a photogenerated valence-band hole and an occupied donor level, probably associated with a Sn²⁺ ion situated roughly 1.4 eV above the valence-band edge.

1. Introduction

Main-group ions with ns^2 electronic configuration, such as Tl⁺, Pb²⁺, Sb³⁺, Bi³⁺, and Au⁻, are well-known for their luminescent properties. As a rule, they exhibit strong absorption in the ultraviolet (UV) with emission in the UV and visible regions of the spectrum.¹ They are among the more interesting classes of luminescent ions, because both the absorption and the emission are highly sensitive to changes in the crystal environment of the ns^2 ion. Considerable research has been devoted to the study of luminescence properties of such ions when doped into insulating hosts, in part due to their technological importance. Some important examples include NaI:Tl⁺, which is a commercial X-ray scintillation phosphor (emission maximum \approx 415 nm); Bi₄Ge₃O₁₂, which is used as a scintillator in the detection of γ -rays and other high-energy particles (Bi³⁺ emission maximum \approx 480 nm); and Ca₅(PO₄)₃(Cl,F):Sb³⁺, Mn²⁺, which is widely used as a fluorescent lamp phosphor (Sb³⁺ emission maximum \approx 490 nm). The electronic relaxation that leads to luminescence is usually ascribed to a transition from an ns^1np^1 excited state to an ns^2np^0 ground state.² The energy levels of the valence s and p orbitals of the ns^2 ion are sensitive to ligand field effects; consequently, the emission wavelength is sensitive to the local coordination environment of the ns^2 ion. The Stokes shift tends to be large when the

ground-state ion has an asymmetric environment, associated with the stereoactive electron lone-pair distortion commonly seen for ns^2 ions, and the excited state adopts a symmetric environment in the ns^1np^1 configuration. As an example, the Stokes shifts for Bi³⁺ emission from the regular, octahedral dopant sites in the perovskites LaGaO₃:Bi³⁺ and LaInO₃:Bi³⁺ are rather small (roughly 0.75 eV or 6000 cm⁻¹),² whereas the Stokes shift is much larger (2.38 eV or 19 000 cm⁻¹) in LaPO₄:Bi³⁺, where the asymmetric Bi³⁺ environment has been confirmed by EXAFS.³ Large Stokes shifts can also be observed when the luminescence involves relaxation from a so-called D-level excited state. The exact details of the D-level excited state are not completely understood, but it is thought to involve some degree of charge transfer from the luminescent ion to the surrounding host lattice.⁴

Even though the luminescent properties of ns^2 ions have been extensively studied, luminescence in the near-infrared (NIR) region has not been observed. To obtain luminescence in the NIR region, transition-metal ion centers, such as chromium, are typically required.⁵ In this paper, we report the observation of strong room-temperature luminescence at 905 nm in BaSnO₃. The luminescence does not seem to be associated with impurities and seems likely to involve Sn²⁺ ions. In previous reports, the emission wavelengths for the luminescence of Sn²⁺ in oxide

[†] The Ohio State University.

[‡] Oregon State University.

(1) Leverenz, H. W. *An Introduction to Luminescence of Solids*; John Wiley & Sons: New York; Chapman & Hall: London, 1950.
(2) Srivastava, A. M. *Mater. Res. Bull.* **1999**, *34*, 1391.

(3) Van Zon, F. B. M.; Koningsberger, D. C.; Oomen, E. W. J. L.; Blasse, G. *J. Solid State Chem.* **1987**, *71*, 396.

(4) Folkerts, H. F.; Ghianni, F.; Blasse, G. *J. Phys. Chem. Solids* **1996**, *57*, 1659.

(5) For example: Eilers, H.; Hemmerich, U.; Jacobsen, S. M.; Yen, W. M.; Hoffman, K. R.; Jia, W. *Phys. Rev. B* **1994**, *49*, 15505.

hosts have generally fallen in the 300–700 nm range.⁶ Thus, the observed wavelength for luminescence in BaSnO₃ is considerably longer than expected. There have been some previous reports of fluorescence in BaSnO₃;⁷ however, it seems that the study of photoluminescence (PL) in BaSnO₃ has been largely overlooked because of the unexpectedly long emission wavelength. In this Article, we report PL properties of BaSnO₃ and the (Ba_{1-x}Sr_x)SnO₃ ($0 \leq x \leq 1$) solid solution, and we speculate on the origin of this unusual PL.

2. Experimental Section

Samples for the (Ba_{1-x}Sr_x)SnO₃ ($0 \leq x \leq 1$) solid solution were synthesized by solid-state reaction at elevated temperature. SnO₂ (99.9%, Fisher), BaCO₃ (99.4%, Mallinckrodt), and SrCO₃ (99.9+%, Aldrich) were used as reagents. These materials were mixed with ethanol and ground in an alumina mortar and pestle. The mixture was first calcined at 1470 K for 10 h in air to decompose the carbonates. After this initial firing, the products were ground, pressed into pellets, and heated at 1720 K for 15 h in air. Samples of (Ba_{1-x}Sr_x)SnO₃ were synthesized in a similar manner with the reagents SnO₂ (99.9%, Cerac or 99.996%, Alfa), BaCO₃ (99.9%, Cerac), and SrCO₃ (99+%, Alfa). Hydrothermal conditions were also used for the low-temperature synthesis of BaSnO₃. Source materials, BaCl₂·2H₂O (Mallinckrodt) and K₂Sn(OH)₆ (99.9%, Aldrich), were placed with water in a Teflon-lined autoclave and kept at 360 K for 1 day. Small single crystals were obtained; they were collected by filtration, washed twice with water and once with acetone, and then dried at 320 K in air. These crystals were identified as BaSn(OH)₆ from both powder and single-crystal X-ray diffraction (XRD) methods. These hydroxide samples were heated in air at various temperatures for 1 h, leading to loss of water and the formation of BaSnO₃ powder. Powders of BaSn(OH)₆ were also prepared by first dissolving BaCl₂·2H₂O (High Purity Chemicals) and SnCl₄·5H₂O (98%, Alfa) in deionized water (0.6 M in each cation) and then adding to an equivalent volume of 8 M NaOH to form a precipitate. The resulting white powder was collected, rinsed several times with deionized water, and dried at 405 K for 2 h. The final product was identified as BaSn(OH)₆ on the basis of XRD measurements. The chemical composition of the samples was also confirmed by using energy-dispersive X-ray analysis (EDX). The phase purity was confirmed, and a structure analysis was completed with laboratory X-ray powder diffraction (XRPD). A Bruker D8 diffractometer (40 kV, 50 mA) was used to collect the XRPD data. It is equipped with a Braun linear position sensitive detector and an incident beam Ge 111 monochromator for selection of Cu K α_1 radiation. The Rietveld method,⁸ as implemented in the TOPAS software package,⁹ was used for the structural analysis of the XRPD data. UV–Vis–NIR diffuse reflectance data were collected over the spectral range 240–2600 nm with a Perkin-Elmer Lambda 900 double-beam spectrometer with MgO as the reference material. The data were transformed into absorbance with the Kubelka–Munk function. For characterization of defect centers, electron spin resonance (ESR) spectra were collected at 300 and 110 K with a Bruker ESP300 X-band spectrometer. The *g* values of signals were calibrated by using the signal of DPPH (*g* = 2.0036) as an internal standard.

PL measurements were made with an Oriel 300 W Xe lamp and a Cary model-15 prism monochromator for excitation. For detection, emitted light was passed through an Oriel 22500 1/8-m monochromator and monitored with a Hamamatsu R636 photomultiplier tube (PMT) over the range 400–950 nm, and a Hamamatsu R1767 PMT over the range 700–1200 nm. Each spectrum was corrected for the throughput

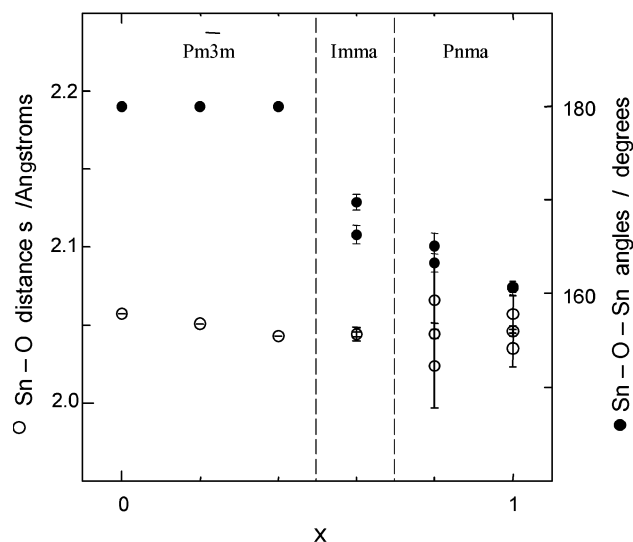


Figure 1. Sn–O–Sn angles (●) and Sn–O distances (○) across the (Ba_{1-x}Sr_x)SnO₃ solid solution as determined from refinements of X-ray powder diffraction data.

and response of the system with Rhodamine B and a standardized W lamp. Variable-temperature spectra were recorded by using a Cryo Industries R102 flow cryostat equipped with a Conductus temperature controller. Lifetime data were obtained with a Q-switched, Quanta-Ray Nd:YAG laser equipped with a frequency-mixing crystal to provide excitation at 355 nm; the pulse width (fwhm) of the laser was measured as 10 ns. The sample emission signal was detected with a PMT that was connected to a 500-MHz Tektronix digital oscilloscope (model TDS350) and interfaced to a PC for data collection. Emission lifetimes were determined from natural log plots of the decay curves.

3. Results

X-ray powder diffraction and EDX measurements confirm that single-phase perovskite samples can be successfully prepared for the entire (Ba_{1-x}Sr_x)SnO₃ solid solution via conventional solid-state synthetic methods.¹⁰ Those samples that are rich in Ba as well as the SrSnO₃ sample are white, while the $x = 0.6$ and 0.8 samples have a dull yellow color. As the size of the alkaline-earth cation decreases, the space-group symmetry evolves from *Pm* $\bar{3}$ *m* ($x = 0, 0.2, 0.4$) to *Imma* ($x = 0.6$) to *Pnma* ($x = 0.8, 1.0$). The symmetry lowering is caused by tilting of the Sn⁴⁺-centered octahedra in response to the increasing mismatch in the fit of the alkaline earth cation to the dodecahedral cavity in the corner-sharing octahedral network. This effect is very common and well understood in perovskites.¹¹ The Rietveld refinement results are summarized in the Supporting Information. Figure 1 shows how the average Sn–O–Sn bond angle increasingly distorts away from the linear bond found in the cubic structure, as the Sr content is increased beyond 0.4. Figure 1 also shows how the Sn–O bond distance remains fairly constant as Sr²⁺ replaces Ba²⁺. It is not clear if the dispersion in Sn–O bond distances for the $x = 0.8$ and 1.0 samples is real or an artifact of the refinements. These samples maintain a high degree of pseudocubic symmetry in the orthorhombic structures, which tends to limit the accuracy of the refinements. Neutron powder diffraction refinements of SrSnO₃ yield Sn–O distances of $2 \times 2.0455(2)$, $2 \times 2.0527(2)$, and $2 \times 2.0627(2)$ Å.¹² It should also be noted that even though the

(10) Smith, A. J.; Welch, A. J. E. *Acta Crystallogr.* **1960**, *13*, 653.

(11) Woodward, P. M. *Acta Crystallogr., Sect. B* **1997**, *53*, 44.

(6) For example: Miyata, T.; Nakatani, T.; Minami, T. *J. Lumin.* **2000**, *87–89*, 1183.

(7) For example: Wilke, K.-Th. *Z. Phys. Chem. (Leipzig)* **1958**, *208*, 361.

(8) Young, R. A. *The RIETVELD Method*; Oxford University Press: London, 1995.

(9) Cheary, R. W.; Coelho, A. A. *J. Appl. Crystallogr.* **1992**, *25*, 109.

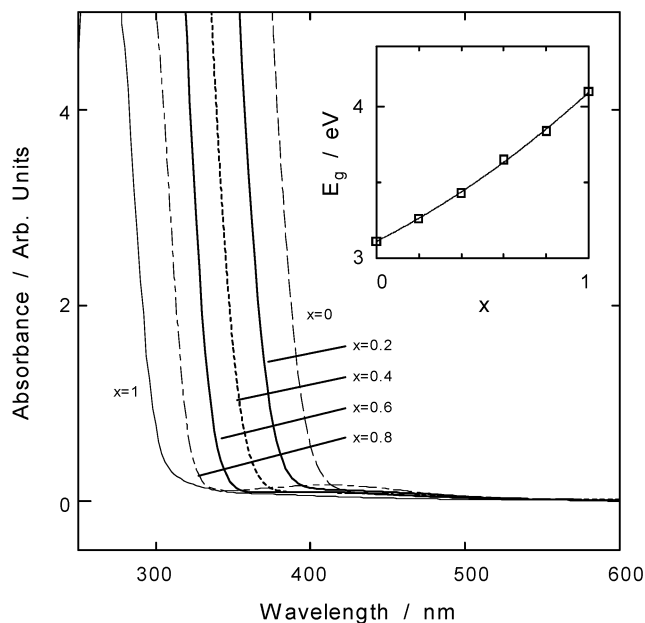


Figure 2. Optical absorption spectra of $(\text{Ba}_{1-x}, \text{Sr}_x)\text{SnO}_3$ at 300 K. The inset shows the estimated band-gap values as a function of x .

$x = 0.2$ and 0.4 samples have a cubic structure on average, recent studies have shown in such perovskite solid solutions there is local distortion and octahedral tilting in response to the partial substitution of a smaller cation on the A-site, even though it does not show up in the average crystal structure.¹³

The optical absorbance, as measured by diffuse reflectance spectroscopy, and the optical band-gap values extracted from these spectra are shown in Figure 2. BaSnO_3 is a semiconductor with an indirect band gap of 3.1 eV, whereas SrSnO_3 has a larger band gap of 4.1 eV.¹⁴ The samples with $x = 0.6$ or 0.8 exhibit a weak absorption around 3 eV, which gives rise to the yellowish appearance. The origin of this feature is not fully understood, although the yellowish tinge can be removed by treatment in H_2 . The band gap of the solid solution changes systematically as a function of Sr^{2+} content, while the unit-cell volume approximately obeys Vegard's law. The band-gap increase can be traced to the effects of octahedral tilting. In BaSnO_3 , the conduction-band minimum is predominantly non-bonding Sn 5s in character, due to the translational symmetry restrictions of the cubic perovskite structure. Octahedral tilting lowers the symmetry to orthorhombic and distorts the linear Sn–O–Sn bonds. As the Sn–O–Sn bonds become increasingly bent, the Sn 5s nonbonding character of the conduction-band minimum is lost and antibonding Sn 5s–O 2p contributions become increasingly important. This pushes up the energy of the conduction-band minimum, resulting in a narrowing of the conduction band and a corresponding increase in the band gap. Details of this mechanism have been described in greater detail in a recent publication.¹⁴

PL spectra for $(\text{Ba}_{1-x}\text{Sr}_x)\text{SnO}_3$ at 300 K are given in Figure 3a. The PL is most intense in BaSnO_3 , which exhibits a broad, strong luminescence centered at 905 nm. The emission peak tails to approximately 760 nm; no PL can be visually observed.

The Stokes shift is 1.9 eV, and the lifetime ranges from 7 to 18 ms, depending on method and temperature of preparation. These extraordinarily long values suggest that the luminescence involves a defect state(s). As x increases, the central wavelength of luminescence shifts to longer wavelengths, reaching a value of 970 nm in SrSnO_3 . It is somewhat surprising to see a red shift of the luminescence peak at the same time that the band gap is steadily increasing. Obviously this leads to a significant increase in the Stokes shift. At the same time, the luminescence intensity decreases to roughly 10% of the value seen in BaSnO_3 ; normalized excitation spectra are shown in Figure 3b. The shift to higher excitation energies with increasing Sr content mirrors that of the band-gap variation shown in the inset of Figure 2. The correspondence between these two results implies that the initial excitation is a transition from the valence to the conduction band.

Luminescence spectra for BaSnO_3 at various temperatures are provided in Figure 4. The intensity of the 905 nm peak decreases as the temperature decreases. Below 190 K, both sharp and broad peaks appear in the visible region near 595 nm. Unlike the NIR luminescence, the intensity of the visible PL peak increases with decreasing temperature, so that at 77 K its integrated intensity is approximately 40% of that of the NIR band. Assuming a minimal change in the optical band gap with temperature, the Stokes shift of the NIR PL peak increases by roughly 0.6 eV upon cooling from 300 to 77 K.

The cubic cell edge and crystallite size of BaSnO_3 samples made by thermal decomposition of the hydrothermal $\text{BaSn}(\text{OH})_6$ crystals¹⁵ are shown in Figure 5. As the annealing temperature increases, the unit-cell edge decreases systematically, while the crystallite size steadily increases. The crystallite size was estimated from the peak broadening seen in the XRPD patterns. Numerical estimates of the size and strain were obtained by fitting the peak shapes with fundamental parameters⁹ in the course of carrying out the Rietveld refinements. The accuracy of the crystallite size values degrades as the crystallite size increases beyond 100–200 nm. The crystallite size and unit-cell edge attain values similar to those of samples made via solid-state reaction upon annealing above 1270 K. The evolution of the unit-cell edge with increasing decomposition temperature agrees with the very recent report by Buscaglia et al. on $\text{BaSn}(\text{OH})_6$ made by wet-chemical processing.¹⁶ The crystallite size increased with the annealing temperature. In terms of the optical properties, we note that the hydrothermal $\text{BaSn}(\text{OH})_6$ samples exhibit luminescence only when the decomposition is carried out above 1270 K, whereas for the directly precipitated $\text{BaSn}(\text{OH})_6$ powders, luminescence is observed from samples decomposed at temperatures as low as 775 K. All of the samples derived from the hydroxide precursor and heated for 1 h exhibit a luminescence brightness that is approximately 25% of that of the samples prepared by solid-state methods. After the BaSnO_3 materials derived from $\text{BaSn}(\text{OH})_6$ are annealed for 5 h at 1573 K, the luminescence brightness exceeds that observed for the solid-state preparations without any noticeable change in particle size or shape. These results indicate that the NIR luminescence in BaSnO_3 is a bulk rather than surface phenomenon, because

(12) Green, M. A.; Prassides, K.; Day, P.; Neumann, D. A. *Int. J. Inorg. Mater.* **2000**, *2*, 35.

(13) Atfield, J. P. *Chem. Mater.* **1998**, *10*, 3239.

(14) Mizoguchi, H.; Eng, H. W.; Woodward, P. M. *Inorg. Chem.* **2004**, *43*, 1667.

(15) The room-temperature crystal structure of $\text{BaSn}(\text{OH})_6$ was determined using single-crystal X-ray diffraction methods. The space group is $P2_1/n$, and the unit-cell dimensions are $a = 9.393 \text{ \AA}$, $b = 6.344 \text{ \AA}$, $c = 10.568 \text{ \AA}$, $\beta = 113.21^\circ$. The details will be published elsewhere.

(16) Buscaglia, M. T.; Leoni, M.; Viviani, M.; Buscaglia, V.; Martinelli, A.; Testino, A.; Nanni, P. *J. Mater. Res.* **2003**, *18*, 560.

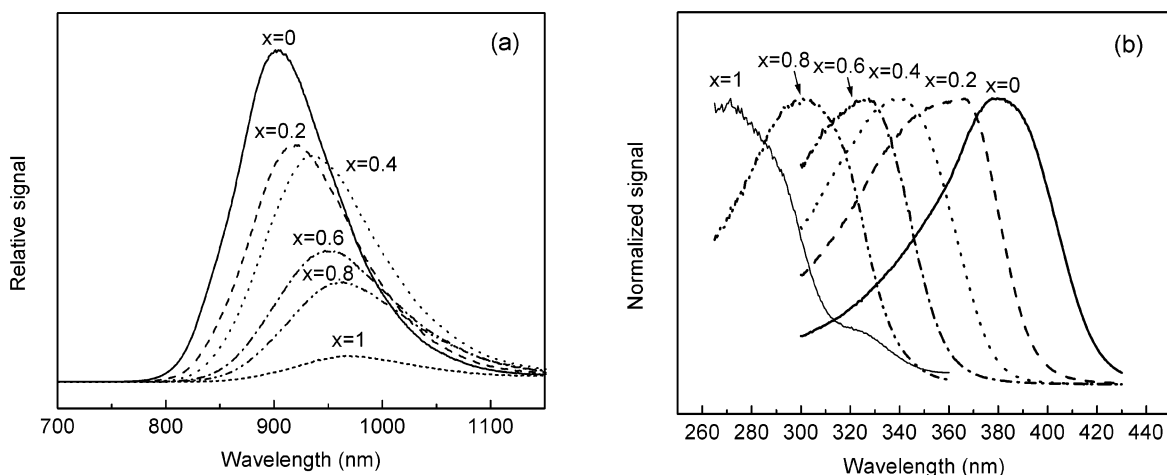


Figure 3. (a) Luminescence spectra and (b) excitation spectra of $(\text{Ba}_{1-x}\text{Sr}_x)\text{SnO}_3$ at 300 K.

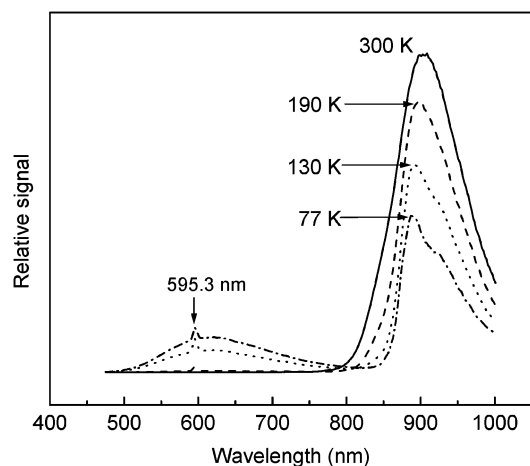


Figure 4. Luminescence spectra of BaSnO_3 , made by solid-state reaction methods, as a function of temperature.

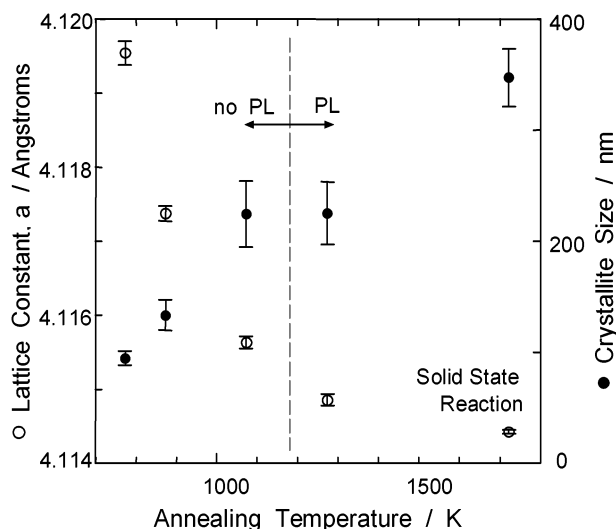


Figure 5. The cubic cell edge (○) and crystallite size (●) for BaSnO_3 samples made by the thermal decomposition of $\text{BaSn}(\text{OH})_6$, as a function of annealing temperature. The sample annealed at 1720 K was made by solid-state reaction.

its emission intensity is not a function of its particle size; particles prepared at 1720 K by solid-state methods are larger than those prepared at 1520 K, but they exhibit similar emission intensities. The fact that high-temperature annealing is needed

to produce samples with a high PL brightness suggests that the samples should be very slightly reduced to show room-temperature PL.

The lack of PL in BaSnO_3 samples prepared from thermal decomposition of $\text{BaSn}(\text{OH})_6$ precursors prepared at temperatures lower than 1270 K could be related to the presence of carbonate ions. The decrease of the unit-cell parameter as the annealing temperature is increased was also reported by Buscaglia et al.¹⁶ for samples prepared by wet-chemical processing. Infrared measurements on powders dispersed in KBr pellets were carried out to better understand the extent and details of thermal decomposition of $\text{BaSn}(\text{OH})_6$. The BaSnO_3 sample prepared at 770 K possessed an intense absorption band near 1425 cm^{-1} that is characteristic of the carbonate C–O stretching mode. As the decomposition temperature increased, the intensity of this peak gradually decreased (see spectra in Supporting Information). It should be noted that the Ba^{2+} ion is known to have an affinity for the CO_3^{2-} ion.

ESR measurements on BaSnO_3 powders were carried out at 300 and 110 K to probe for the formation of the luminescence center at various thermal decomposition temperatures. Signals due to Mn^{2+} or Cr^{3+} ions, which are known to be luminescent centers, were not detected. However, the sample made at 1720 K did show a very weak signal that we attribute to Mn^{4+} . The presence of manganese is thought to originate from one of the furnaces used for synthesis, judging from the fact that the sample made at 1470 K in a different furnace did not contain the Mn^{4+} ESR signal. To investigate the possibility that manganese contamination might be linked to the photoluminescence in some way, $\text{BaSn}_{1-x}\text{Mn}_x\text{O}_3$ ($x = 0.001, 0.005, 0.01, \text{ and } 0.02$) samples were intentionally prepared. These samples did not show any NIR luminescence. $\text{BaSn}_{1-x}\text{Cr}_x\text{O}_3$ ($x = 0.01 \text{ and } 0.02$) was also prepared and was found not to exhibit photoluminescence at room temperature. The possibility of Al^{3+} contamination (from the alumina mortar and pestle or the crucibles) was also investigated. A sample of $\text{BaSn}_{0.995}\text{Al}_{0.005}\text{O}_3$ was also prepared and was found not to exhibit photoluminescence at room temperature.

4. Discussion

Let us consider the origins of luminescence in BaSnO_3 and its unusually long-wavelength emission at room temperature. The fact that luminescence is only observed in samples treated

at high temperature, along with the long lifetime of the excited state, suggest that strong room-temperature PL is associated with a defect in the material. Furthermore, the large Stokes shift is not consistent with self-luminescent exciton recombination, and there is no evidence to suggest that extrinsic impurities are responsible for the luminescence either. In addition to the ESR and doping studies that seem to rule out the possible role of Mn^{2+} and Cr^{3+} , we found almost identical luminescence from BaSnO_3 samples prepared in four different manners: (a) samples prepared at Ohio State University from 99.9% purity SnO_2 , (b) samples prepared at Oregon State University from 99.996% purity SnO_2 , (c) samples prepared from high-temperature annealing of single-crystal $\text{BaSn}(\text{OH})_6$ precursors, and (d) samples prepared from precipitated $\text{BaSn}(\text{OH})_6$ powders. Therefore, we conclude that the unusual luminescence in the NIR region originates from an intrinsic defect center or centers in BaSnO_3 . The most likely scenario is that high-temperature annealing creates oxygen vacancies, which are at least partially charge compensated by the creation of reduced Sn^{n+} sites ($n < 4$).

An important distinction between BaSnO_3 and other materials containing Sn^{2+} luminescent centers is the fact that BaSnO_3 is a semiconductor rather than an insulator. Reasonably good electronic conductivity has been observed in n-doped $\text{BaSn}_{1-x}\text{Sb}_x\text{O}_3$ samples.¹⁷ This fact raises the possibility that the luminescent behavior of BaSnO_3 is based on a mechanism different from intra-atomic excitation and recombination of an isolated ns^2 ion in an insulating host. As the value of x increases across the $(\text{Ba}_{1-x}\text{Sr}_x)\text{SnO}_3$ solid solution, the changes in the band gap, as measured by diffuse reflectance methods (Figure 2), correspond very well to changes in the PL excitation wavelength (Figure 3b). This observation is strong evidence that the electronic excitation that ultimately leads to PL is excitation of an electron from the valence to the conduction band, particularly on the Ba-rich side of the solid solution. From this observation, it is not unreasonable to infer that the PL observed in BaSnO_3 may have similarities to the behavior of classic semiconductor phosphors such as $\text{ZnS}:\text{Cu}^+$ or $\text{ZnS}:\text{Ag}^+$, where the radiative transition is from the conduction band into an impurity-based acceptor level located in the band gap. Application of this model to the $\text{Ba}_{1-x}\text{Sr}_x\text{SnO}_3$ system is not consistent with the observation that strontium substitution increases the band gap significantly, while at the same time leading to a red shift in the emission spectrum. However, a blue shift in the emission line would not necessarily be expected if the luminescence involves radiative recombination of a valence-band hole and an occupied donor level located in the gap, such as Sn^{2+} . It is known that the increase in band gap for ASnO_3 perovskites can be traced primarily to a decrease in the width of the conduction band, in response to octahedral tilting.¹⁴ Therefore, it is realistic to expect that the valence-band maximum will remain largely O 2p nonbonding and at roughly the same energy level. Furthermore, the occupied 5s orbital of a Sn^{2+} ion would be expected to fall in the band gap. Density functional theory calculations show that in SnO the occupied Sn 5s–5p hybrid states fall at an energy roughly ~ 1.0 eV above the top of the O 2p band,¹⁸ so that a Sn^{2+} 5s \rightarrow VB emission at a wavelength of ~ 1.4 eV is of the right order of magnitude for such a radiative recombination process. The decreased PL efficiency that occurs either on doping with Sr^{2+} (Figure 3a) or on lowering the temperature

could originate from the reduced carrier mobility that would result from bending the Sn–O–Sn bonds in the former case and from a model based on polaronic hole transport in the latter case. Another piece of evidence consistent with this model is the observation that purposely n-doped $\text{BaSn}_{1-x}\text{Sb}_x\text{O}_3$ exhibits negligible room-temperature luminescence. One questionable feature of this hypothesis is the fact that hole mobility in such oxides is normally quite small. However, the positively charged hole will be attracted to the negative site potential of a Sn^{2+} ion on a Sn^{4+} site, and it is conceivable that only holes generated within a few jumps of an Sn^{2+} center contribute to the PL. The need for a photogenerated hole to migrate to and recombine with a Sn^{2+} center is consistent with the long lifetime.

The origin of the low-temperature emission centered at 595 nm is not clear. One possibility is that the peak at 595 nm in BaSnO_3 may originate from self-trapped exciton luminescence associated with isolated Sn^{2+} centers¹⁹ or those associated with oxygen vacancies. However, the relatively long wavelength of the visible emission casts considerable doubt on this assignment. Another possibility is that this PL is associated with conduction-band electrons trapped on oxygen-vacancy sites. Measured decay curves in this emission region cannot be fit with a single exponential, but a fast component of 10 μs is observed.

5. Conclusion

In conclusion, further study is needed to conclusively determine the origin of the interesting PL in BaSnO_3 . There can be no doubt, however, that strong room-temperature near-IR luminescence occurs in this material. Photoluminescence in the near-IR is a very unusual feature among oxides containing main-group ions. The initial characterization points toward a model based on recombination of a photogenerated valence-band hole and an occupied donor level situated roughly 1.4 eV above the valence-band edge. This type of oxide semiconductor luminescence based on hole recombination is rare. It would seem to be favored in this case by the high covalency of the Sn^{4+} –O bond and the linear O–Sn–O geometry. Furthermore, it is rare to find a material that can be doped so as to become either an electrical conductor or a strongly luminescent material. This opens the possibility that NIR electroluminescent thin-film devices based on BaSnO_3 – BaSnO_{3-x} – $\text{BaSn}_{1-x}\text{Sb}_x\text{O}_3$ heterostructures could be constructed. The lattice matching would be excellent, and it is possible that efficient devices could be fabricated.

Acknowledgment. We thank Dr. C. Turro for help with the photoluminescence measurements, Dr. G. D. Renkes for help with the XRD and ESR measurements, Dr. R. L. McCreery and A. M. Nowak for help with the use of a spectrophotometer at Ohio State University, and Dr. J. Gallucci for help with the single-crystal analysis. We also thank D. Podkoscielny for the synthesis of two of the BaSnO_3 samples and Dr. J. W. Nibler for assistance with the lifetime measurements.

Supporting Information Available: Crystal structure data obtained from the analysis of X-ray powder diffraction data for $\text{Ba}_{1-x}\text{Sr}_x\text{SnO}_3$ samples and IR spectra (PDF). This material is available free of charge via the Internet at <http://pubs.acs.org>.

JA048866I

- (17) Larramona, G.; Gutierrez, C.; Pereira, I.; Nunes, M. R.; da Costa, F. M. A. *J. Chem. Soc., Faraday Trans. 1* **1989**, 85, 907.
- (18) Watson, G. W. *J. Chem. Phys.* **2001**, 114, 758.
- (19) Donker, H.; Smit, W. M. A.; Blasse, G. *Phys. Status Solidi B* **1988**, 148, 413.